Quantitative analysis of large axonal fibres in the CST

To evaluate the degeneration of axonal fibres in the CST, we calculated the density of axonal fibres in the lateral column of the spinal cord. Specimens corresponding to the C5–6 levels were prepared for all of the patients and 13 controls. For this assay, the paraffin-embedded spinal cords were immunostained using the anti-pNF antibody and diaminobenzidine as chromogen without additional nuclear staining to visualise only axons as brown particles. The microscopic views were binarised and automatically recognised using Luzex AP software (Nireco, Tokyo, Japan) that was coupled to the microscope via a CCD video camera. This software automatically measured the particle counts and diameters on the binarised pictures.[13] Axonal counts were evaluated on five areas of 10 000 μm^2 (×40 objective) randomly chosen from the CST of the spinal lateral column in each patient and averaged. To validate duplicability between tests, we constructed two axon size histograms from 13 ipsilateral control samples (see online supplementary file). Briefly, the variability between the test and retest was sufficiently small to count the axons for each axon size. We constructed a histogram of axonal sizes in the CST (figure 2A), and the density of the large axons (axonal fibres/10 000 μm^2) was calculated (figure 2B,C) for patients with PMA and ALS and control samples.

Statistical analysis

The demographic features of patients with PMA and ALS were compared using the Mann-Whitney U test for continuous variables or the Pearson's χ^2 test or Fisher's exact test to assess bivariate correlations. The Kruskal-Wallis test was used for analyses between three groups, and the t test was used for analyses between two groups. The significance level was set at a p value of 0.05 for comparisons between two groups and 0.016 for comparisons between three groups. All of the statistical tests performed were two-sided and were conducted using the software program PASW V.18.0 (IBM SPSS).

RESULTS

Demographic features of the registered patients

The included patients consisted of 67 men and 40 women. The mean age at disease onset was 62.7 ±12.4 years, and the median duration from disease onset to death was 27 months (range 2–348 months). Seventeen patients were treated with tracheostomy positive-pressure ventilation (TPPV). Initial symptoms included upper limb weakness in 40.2%, lower limb weakness in 32.7%, bulbar symptoms in 24.3% and respiratory symptoms in 2.8% of the included patients. Fourteen (13.1%) patients were categorised into the clinical PMA group, and 93 (86.9%) patients were

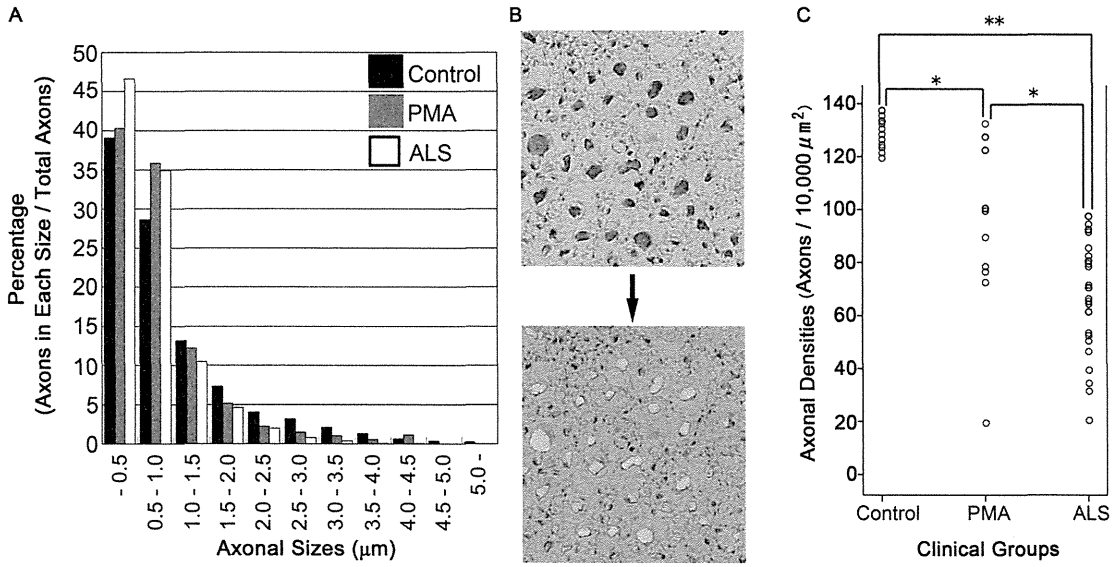

Figure 2 Quantitative analysis of the axonal fibres in the corticospinal tract. (A) Phosphorylated neurofilament (pNF)-positive fibres were automatically binarised using Luzex AP software. The density of pNF-positive axons (particles/10 000 μm^2) was automatically calculated using averaged data from five fields (×400). The histogram of axonal sizes revealed that the percentages of axons that were more than 1 μm in diameter were smaller in ALS and PMA than in controls. (B) The large axonal fibres more than 1 μm in diameter were automatically recognised, binarised and counted using the software to successfully evaluate the axonal density. (C) There were significant differences in the densities of axons that were more than 1 μm in diameter between all pairs of clinical groups: p=0.001 (*) between the clinical amyotrophic lateral sclerosis (ALS) and clinical progressive muscular atrophy (PMA) groups, p=0.001 (*) between the clinical PMA and control groups and p<0.001 (**) between the clinical ALS and control groups. All patients diagnosed with clinical ALS exhibited lower values than the controls. In contrast, the results of the clinical PMA group were widely diverse, ranging from low values to values within the normal range.

classified into the clinical ALS group. With regard to clinical diagnosis, 10 (71.4%) of 14 patients with clinical PMA and 88 (94.6%) of 93 patients with clinical ALS were correctly diagnosed as PMA or ALS by the first referred physicians. However, one patient with clinical PMA and four patients with clinical ALS were initially diagnosed as having cervical or lumbar canal stenosis based on focal weakness restricted to one upper or lower limb and canal stenosis on MRI. One of the patients with clinical PMA was initially diagnosed as having carpal tunnel syndrome based on weakness restricted to the distal area of the median nerve in the right hand. One of the patients with clinical PMA was diagnosed as having polyradiculopathy because the cauda equina was slightly enhanced on gadolinium-enhanced MRI. One of the patients with clinical PMA was initially diagnosed as having myositis based on myalgia and slight lymphatic infiltration on a muscle biopsy. One of the patients with clinical ALS was initially diagnosed as having parkinsonian syndrome because the patient showed bradykinesia due to marked rigospasticity in the limbs. The demographic features of patients with clinical PMA and ALS are presented in table 1. In summary, no significant differences in the age at onset, male-to-female ratio, clinical duration (whether including or excluding the TPPV treatment period) or initial symptoms were detected between the clinical PMA and ALS groups.

Pathological evaluations

Degeneration in the UMN system

Loss of Betz cells in the primary motor cortex

Ten (76.9%) of the 13 patients with clinical PMA exhibited a loss of Betz cells, which was severe in 3 (23.1%) of these patients (figure 3). However, in 2 (15.4%) of the 13 patients with clinical PMA, no loss of Betz cells or gliosis in the primary motor cortex was detectable. In contrast, all of the patients diagnosed with clinical ALS exhibited a loss of Betz cells, which was severe in 10 (34.5%) of the 29 patients with clinical ALS. There was no significant difference in the severity of this pathological change between the clinical groups.

Aggregation of macrophages in the primary motor cortex

The aggregation of CD68 macrophages in the primary motor cortex was detected in 10 (76.9%) of the 13 patients with clinical PMA. In contrast, all of the patients diagnosed with clinical ALS exhibited the aggregation of macrophages in the primary motor cortex. When comparing the clinical groups, this pathological change was significantly more severe in clinical ALS than clinical PMA ($p=0.048$).

CST degeneration

Myelin pallor was present in 8 (61.5%) of the 13 patients with clinical PMA. The aggregation of macrophages within the CST was detected in 11 (84.6%) of the 13 patients with clinical PMA. In the clinical ALS group, all patients exhibited myelin pallor and macrophage aggregation in the CST. When comparing the clinical groups, this pathological change was significantly more severe in clinical ALS than clinical PMA ($p=0.004$).

Degeneration in the LMN system

All of the patients diagnosed with either clinical PMA or ALS exhibited neuronal loss in the spinal anterior horns (figure 3). This neuronal loss was severe in 11 (84.6%) of the 13 patients with clinical PMA and 20 (69%) of the 29 patients with clinical ALS. All of the patients diagnosed with clinical PMA and 27 (93.1%) of the 29 patients with clinical ALS exhibited neuronal loss in the cranial nerve nuclei. This neuronal loss was severe in 6 (46.2%) of the 13 patients with clinical PMA and 11 (37.9%) of the 29 patients with clinical ALS. When comparing the clinical groups, there was no significant difference in the severity of LMN loss. Eight (61.5%) of the 13 patients with clinical PMA and 24 (82.8%) of the 29 patients with clinical ALS displayed Bunina bodies in the LMN system.

Table 1 Demographic features of clinical patients with PMA and ALS

	Clinical PMA	Clinical ALS	p Value
Number of patients	14	93	
Age at onset (years, mean±SD)	60.8±10.8	63.0±12.7	0.388*
Male/female	10/4	57/36	0.563†
Duration from onset to death (months; median, range)‡	21 (5–192)	29 (2–348)	0.764*
Initial symptoms (number of patients)			
Bulbar symptoms	3 (21.4%)	23 (24.7%)	0.738†
Upper limb weakness	5 (35.7%)	38 (40.9%)	0.738†
Lower limb weakness	5 (35.7%)	30 (32.3%)	0.738†
Respiratory symptoms	1 (7.1%)	2 (2.2%)	

*Mann-Whitney U test.
†Fisher's exact test.
‡Including the TPPV treatment period.
ALS, amyotrophic lateral sclerosis; PMA, progressive muscular atrophy; TPPV, tracheostomy positive-pressure ventilation.

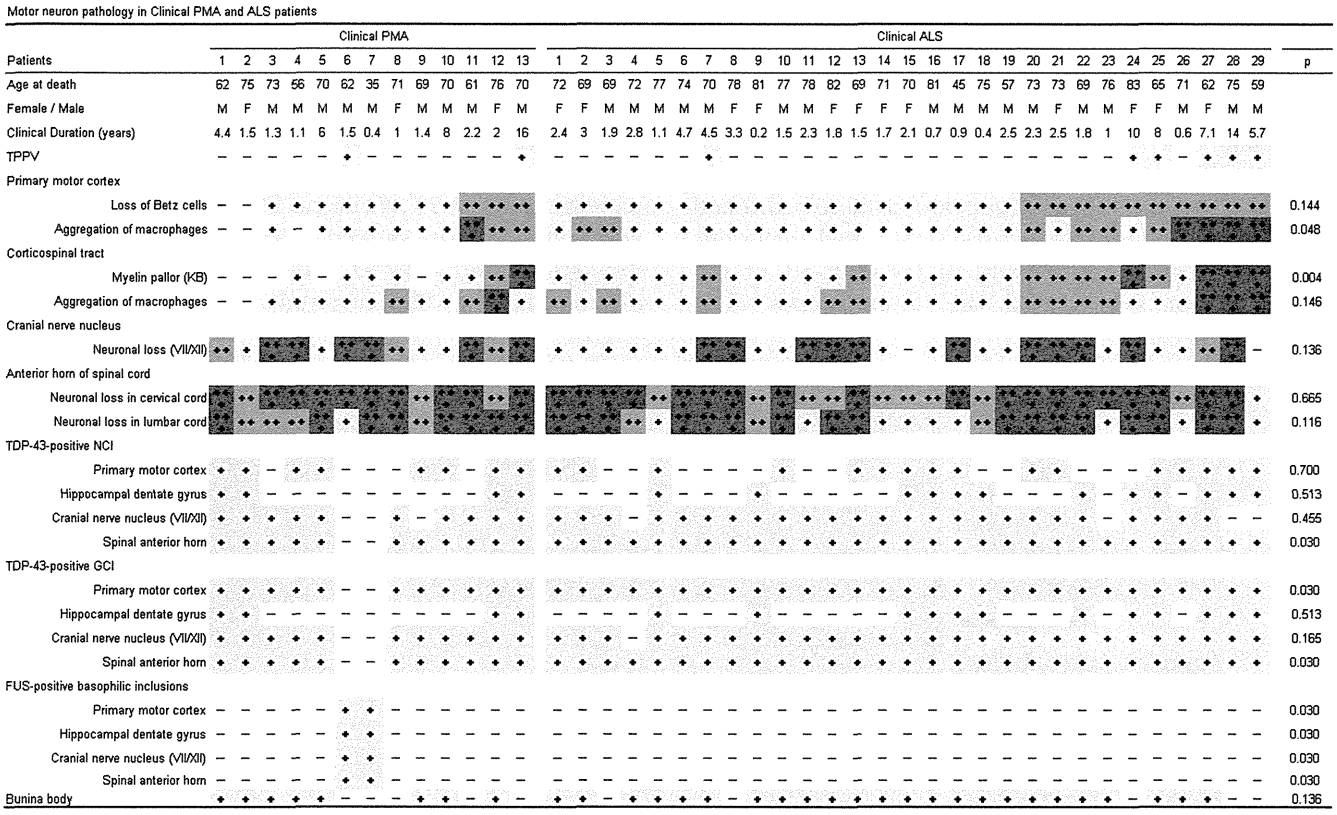

Figure 3 Summary of the neuropathological findings in the included patients. The stages of the pathological changes correspond to those in figure 1. Pathological changes between the clinical groups were compared using Pearson's χ^2 test. ALS, amyotrophic lateral sclerosis; FUS, antifused-in-sarcoma; GCI, glial cytoplasmic inclusions; KB, Klüver-Barrera staining; NCI, neuronal cytoplasmic inclusion; PMA, progressive muscular atrophy; TDP-43, 43 kDa TAR DNA-binding protein; TPPV, tracheostomy positive-pressure ventilation.

Immunohistochemical profiles

In 11 (84.6%) of the patients with clinical PMA, we detected ubiquitin and TDP-43-positive neuronal cytoplasmic inclusions (NCIs) in the LMN system (figure 3). In eight of these patients, TDP-43-positive NCIs were also detected in the primary motor cortex. All of the patients with clinical ALS displayed ubiquitin and TDP-43-positive NCIs in the LMN system. Moreover, TDP-43-positive glial cytoplasmic inclusions were observed in the spinal anterior horn and primary motor cortex in all of the TDP-43-positive patients of the clinical ALS and PMA groups. In contrast, two of the patients with clinical PMA (15.4%) exhibited basophilic inclusion bodies in the neuronal cytoplasm, which were broadly extended throughout the central nervous system. These inclusions were positive for FUS but negative for TDP-43, α-internexin and peripherin.

Quantitative analysis of large axonal fibres in the CST

The histogram of axonal sizes revealed that the percentage of axons that were greater than 1 μm in diameter was smaller in ALS (18.5%) and PMA (23.9%) than in controls (32.3%), resulting in a relative increase in the percentage of smaller axons (figure 2). Then, we measured the densities of large axons that were greater than 1 μm in diameter. The average densities were as follows: clinical ALS, 68.3±20.9 fibres/10 000 μm^2; clinical PMA, 97.2±31.5 fibres/10 000 μm^2 and controls, 129.1±6.1 fibres/10 000 μm^2 ($p=0.001$ between the clinical ALS and PMA groups; $p=0.001$ between the clinical PMA and control groups; $p<0.001$ between the clinical ALS and control groups). All patients diagnosed with clinical ALS exhibited lower values than the range of normal values that was obtained from the controls. In contrast, the results from the clinical PMA group were widely diverse. The results from 5 (38.5%) of the 13 patients with clinical PMA were within the normal range, but 8 (61.5%) of these patients exhibited lower values than the normal range. One patient with PMA who had been treated with TPPV exhibited an exceptionally low value.

Pathological overview of the patients diagnosed with clinical PMA or clinical ALS

Clinical PMA: 11 (84.6%) of the 13 patients with clinical PMA displayed UMN degeneration (either the loss of Betz cells, myelin pallor or the aggregation of macrophages in the primary cortex or CST) and LMN degeneration. Nine of these patients exhibited TDP-43-positive inclusions and the remaining 2 patients displayed FUS-positive basophilic inclusion bodies. Their large

CST axon densities were diverse, ranging from low values to values within the normal range that were obtained from the control participants. In 2 (15.4%) of the 13 patients with clinical PMA, neuropathological parameters that we defined as UMN system degeneration were all negative. Their large CST axon density was within the normal range. These two patients exhibited abundant TDP-43-positive neuronal and glial inclusions in the LMN and, occasionally, in layers II–III of the primary motor cortex and the hippocampus. The pathological findings from the representative patients are shown in figure 4.

Clinical ALS: All 29 patients displayed a combination of UMN and LMN system degeneration and exhibited TDP-43-positive inclusions.

Additionally, of the respirator-managed patients, three patients (patient 13 of clinical PMA and patients 27 and 28 of clinical ALS) showed diffusely extended neuronal loss, gliosis and TDP-43 pathology beyond the motor neuron systems, which involved all layers of the cerebral

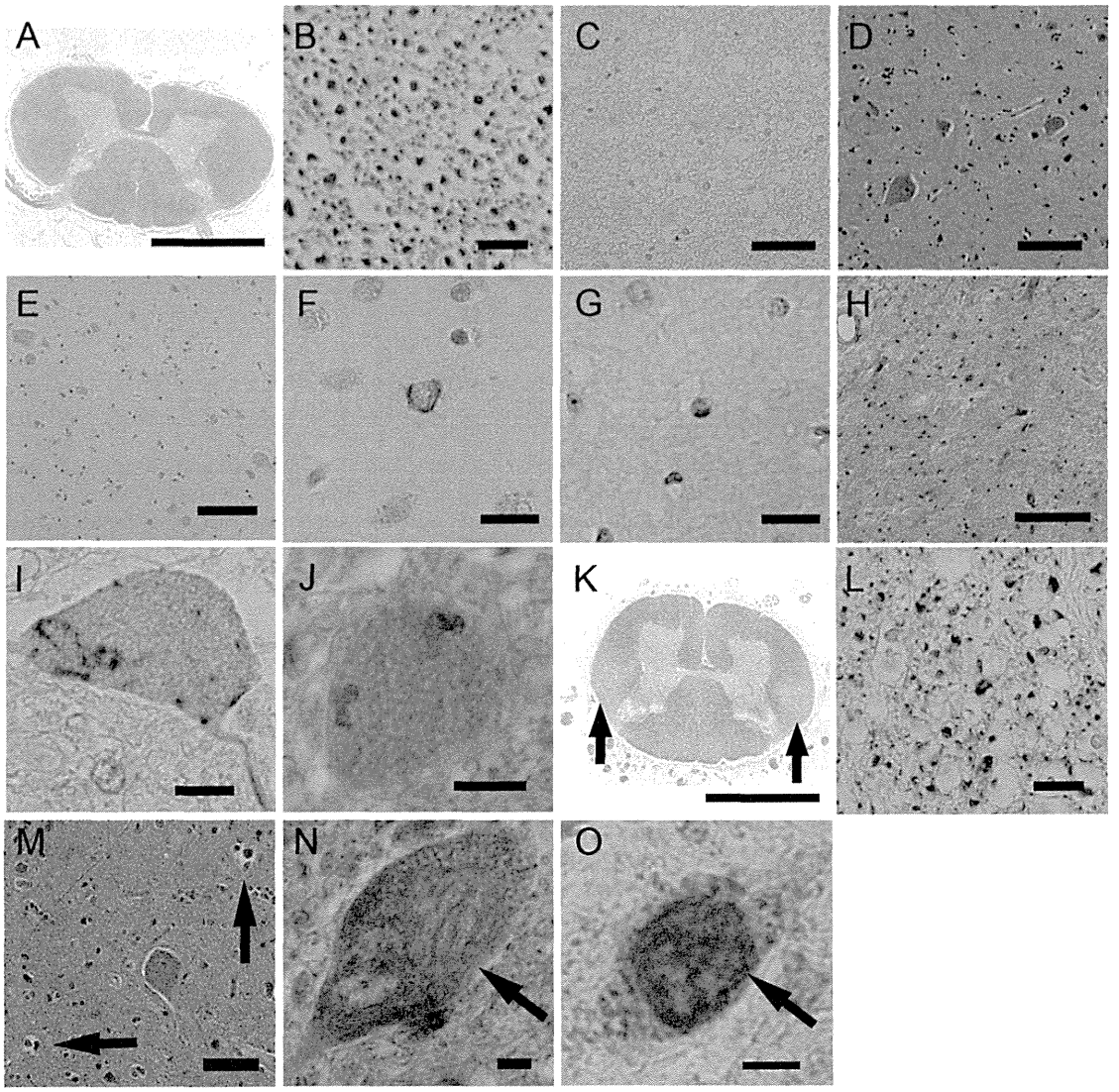

Figure 4 *Neuropathological profiles of the patients in the clinical progressive muscular atrophy group.* (A–J) correspond to patient 2. The corticospinal tracts (CST) did not display myelin pallor (A), loss of large axonal fibres (B), or aggregation of macrophages (C). Additionally, in the primary motor cortex, neither the loss of Betz cells (D) nor aggregation of macrophages (E) was detected. The upper layers of the primary motor cortex rarely contained phosphorylated 43 kDa TAR DNA-binding protein (pTDP-43)-positive neuronal (F) and glial (G) inclusions. The spinal anterior horn displayed severe neuronal loss (H), pTDP-43-positive skein-like inclusions (I) and Bunina bodies (J). (K–M) correspond to patient 12. The CST displayed myelin pallor (K) and the depletion of large axonal fibres (L). Neuronophagia was often found in the primary motor cortex (M, arrows). (N and O) correspond to patient 6. The spinal motor neurons contained basophilic inclusion bodies (N) that were positive for antifused-in-sarcoma (FUS) based on immunohistochemistry (O). (A and K) Klüver-Barrera staining, (B) antiphosphorylated neurofilament immunohistochemistry, (C and E) anti-CD68 immunohistochemistry, (D, H, J and M) H&E staining, (F, G and I) anti-pTDP-43 immunohistochemistry and (O) anti-FUS immunohistochemistry. Scale bars: (A and K) 3 mm, (D and E) 100 μm, (C, H and M) 50 μm, (B) 20 μm and (F, G, I, J, N and O) 10 μm.

neocortices, the striatum, thalamus, cerebellar dentate nucleus and non-motor nuclei in the brainstem, including the substantia nigra, red nucleus, periaqueductal grey matter, inferior olivary nucleus and reticular formation.

DISCUSSION

Our study demonstrated the clinicopathological profiles of patients with clinical PMA and ALS in a consecutive autopsy series. The clinical evaluations in this study revealed rapid disease progression and short survival duration in patients with clinical PMA, which are analogous courses to those that are characteristic of clinical ALS. Contrary to our results, it has been described that PMA exhibits slower progression and longer survival duration compared with ALS.[3] However, recent studies revealed that PMA follows a relentlessly progressive course and that the survival duration is not much longer than that of ALS.[2 4 9 10 14] The relatively small number of patients in our study may have contributed to the absence of significant differences in the survival durations between the clinical PMA and ALS groups.

Our pathological results indicate that, of the patients with clinical PMA, 85% exhibited degeneration in the UMN and LMN systems, which corresponds with ALS. However, the remaining 15% of patients with clinical PMA lacked any apparent degeneration in the UMN system. A previous study reported that approximately 50% of all patients with PMA exhibit macrophages in the CST.[5] Another report demonstrated the degeneration of the pyramidal tract and loss of Betz cells in 65% and 60%, respectively, of the patients diagnosed with the PMA phenotype.[6] Our results revealed that patients with PMA more frequently had degeneration in the UMN system than those reported in previous studies; however, in a few patients with PMA, UMN degeneration remained undetectable at death. Our pathological results revealed differential UMN involvement between patients with PMA and indicated that PMA and ALS are continuous pathological entities. Regarding immunohistochemical aspects, several studies have revealed that TDP-43 pathology is commonly observed in the cerebral cortices or the subcortical grey matter of patients with PMA.[7 8] In our results, TDP-43-positive neuronal or glial inclusions in the motor cortices or hippocampus were common in the clinical ALS and PMA groups and were found even in patients apparently lacking UMN degenerative changes. A recent report described the propagation of TDP-43 pathology in ALS, which starts from the UMN and LMN systems and spreads to the anteromedial temporal lobes through the motor neuron system.[15] Based on this theory of TDP-43 propagation, TDP-43 pathology beyond the LMN system in patients with PMA may support the pathological continuity between these two clinical phenotypes.

The standard diagnostic criteria for ALS are the revised El Escorial criteria, which require a combination of UMN and LMN symptoms/signs for the diagnosis of ALS.[12] However, it is often difficult to clinically determine whether the UMN is involved,[16] which sometimes results in diagnostic difficulty. In our patient series, only 71.4% of the patients with clinical PMA were correctly diagnosed by the first referred physicians, although 94.6% of the patients with clinical ALS were diagnosed correctly. Recently, several studies have demonstrated the utility of radiological procedures, including transcranial magnetic stimulation, ^{1}H MR spectroscopy and diffusion tensor imaging in the detection of UMN system deterioration in a subset of patients with PMA.[14 17–20] Based on our results, a large subset of patients with PMA may have some degree of UMN degeneration. In such patients, these radiological or electrophysiological procedures would be expected to increase the sensitivity of detection of UMN degeneration. However, our results also indicate that some of the patients with PMA exhibit sparse morphological changes in the UMN system, even at death. It may be difficult to detect UMN degeneration using these procedures in such patients. To diagnose clinical patients with PMA displaying sparse UMN degeneration as ALS in the early phase of the disease course may be a future subject of focus.

A limitation of our study was the inability to evaluate the entire motor cortex and CST, and it is controversial whether patients with apparently intact UMN systems actually lack or have extremely mild UMN involvement. Another methodological limitation is that we evaluated axonal sizes and densities using neutral formalin-fixed, paraffin-embedded specimens. The tissues may be somewhat distorted when compared with conventional nerve fixation using glutaraldehyde followed by Epon embedding. Our methods were considered to be appropriate to assess the proportional changes in the sizes of pyramidal axons, but the absolute values of axonal diameters can vary from those that have been obtained using other histological techniques.[13]

In summary, 84.6% of patients with clinical PMA displayed UMN and LMN degeneration, which is consistent with the pathological profiles of ALS. In 15.4% of the patients with clinical PMA, degeneration in the UMN system was undetectable. The large axon density in the CST varied from low values to a normal range. In contrast, all of the clinical patients with ALS displayed a combination of UMN and LMN system degeneration and significantly reduced large axon density in the CST.

Acknowledgements The authors specially thank Dr M Hasegawa, Department of Neuropathology and Cell Biology, Tokyo Metropolitan Institute of Medical Science, for performing the genetic analysis of the fused-in-sarcoma (FUS) genes.

Contributors YR and NA contributed to the conception and design of the study. All of the authors participated in the acquisition, analysis and interpretation of the data. MY and GS drafted the manuscript. MI and HW assisted in writing and editing the manuscript.

Funding This work was supported by Grants-in-Aid from the Research Committee of CNS Degenerative Diseases of the Ministry of Health, Labor, and Welfare of Japan.

Competing interests None.

Ethics approval This study was approved by the ethics committees of Nagoya University and Aichi Medical University.

Provenance and peer review Not commissioned; externally peer reviewed.

Data sharing statement No additional data are available.

REFERENCES

1. Neumann M, Sampathu DM, Kwong LK, *et al.* Ubiquitinated TDP-43 in frontotemporal lobar degeneration and amyotrophic lateral sclerosis. *Science* 2006;314:130–3.
2. de Carvalho M, Scotto M, Swash M, *et al.* Clinical patterns in progressive muscular atrophy (PMA): a prospective study. *Amyotroph Lateral Scler* 2007;8:296–9.
3. Norris FH. Adult progressive muscular atrophy and hereditary spinal muscular atrophies. In: Vinken PJ, Bruyn GW, Klawans HL, De Jong JMBV, eds. *Handbook of clinical neurology: diseases of the motor system.* Vol 59. Amsterdam: North-Holland Publishing Company, 1991:13–34.
4. Visser J, van den Berg-Vos RM, Franssen H, *et al.* Disease course and prognostic factors of progressive muscular atrophy. *Arch Neurol* 2007;64:522–8.
5. Ince PG, Evans J, Knopp M, *et al.* Corticospinal tract degeneration in the progressive muscular atrophy variant of ALS. *Neurology* 2003;60:1252–8.
6. Brownell B, Oppenheimer DR, Hughes JT. The central nervous system in motor neurone disease. *J Neurol Neurosurg Psychiatry* 1970;33:338–57.
7. Geser F, Stein B, Partain M, *et al.* Motor neuron disease clinically limited to the lower motor neuron is a diffuse TDP-43 proteinopathy. *Acta Neuropathol* 2011;121:509–17.
8. Nishihira Y, Tan CF, Hoshi Y, *et al.* Sporadic amyotrophic lateral sclerosis of long duration is associated with relatively mild TDP-43 pathology. *Acta Neuropathol* 2009;117:45–53.
9. Kim WK, Liu X, Sandner J, *et al.* Study of 962 patients indicates progressive muscular atrophy is a form of ALS. *Neurology* 2009;73:1686–92.
10. Van den Berg-Vos RM, Visser M, Kalmijn S, *et al.* A long-term prospective study of the natural course of sporadic adult-onset lower motor neuron syndromes. *Arch Neurol* 2009;66:751–7.
11. Koike H, Hirayama M, Yamamoto M, *et al.* Age associated axonal features in HNPP with 17p11.2 deletion in Japan. *J Neurol Neurosurg Psychiatry* 2005;76:1109–14.
12. Brooks BR, Miller RG, Swash M, *et al.* El Escorial revisited: revised criteria for the diagnosis of amyotrophic lateral sclerosis. *Amyotroph Lateral Scler Other Motor Neuron Disord* 2000;1:293–9.
13. Sobue G, Hashizume Y, Mitsuma T, *et al.* Size-dependent myelinated fiber loss in the corticospinal tract in Shy-Drager syndrome and amyotrophic lateral sclerosis. *Neurology* 1987;37:529–32.
14. Mitsumoto H, Ulug AM, Pullman SL, *et al.* Quantitative objective markers for upper and lower motor neuron dysfunction in ALS. *Neurology* 2007;68:1402–10.
15. Brettschneider J, Del Tredici K, Toledo JB, *et al.* Stages of pTDP-43 pathology in amyotrophic lateral sclerosis. *Ann Neurol* 2013;74:20–38.
16. Swash M. Why are upper motor neuron signs difficult to elicit in amyotrophic lateral sclerosis? *J Neurol Neurosurg Psychiatry* 2012;83:659–62.
17. Sach M, Winkler G, Glauche V, *et al.* Diffusion tensor MRI of early upper motor neuron involvement in amyotrophic lateral sclerosis. *Brain* 2004;127:340–50.
18. Vucic S, Ziemann U, Eisen A, *et al.* Transcranial magnetic stimulation and amyotrophic lateral sclerosis: pathophysiological insights. *J Neurol Neurosurg Psychiatry* 2013;84:1161–70.
19. Graham JM, Papadakis N, Evans J, *et al.* Diffusion tensor imaging for the assessment of upper motor neuron integrity in ALS. *Neurology* 2004;63:2111–19.
20. Prudlo J, Bißbort C, Glass A, *et al.* White matter pathology in ALS and lower motor neuron ALS variants: a diffusion tensor imaging study using tract-based spatial statistics. *J Neurol* 2012;259:1848–59.

NEUROPATHOLOGY

Neuropathology 2014; **34**, 555–570 doi:10.1111/neup.12143

Symposium: Definition and Differentials – How to Distinguish Disease-Specific Changes on Microscopy

Astrocytic inclusions in progressive supranuclear palsy and corticobasal degeneration

Mari Yoshida

Institute for Medical Science of Aging, Aichi Medical University, Aichi, Japan

Tufted astrocytes (TAs) in progressive supranuclear palsy (PSP) and astrocytic plaques (APs) in corticobasal degeneration (CBD) have been regarded as the pathological hallmarks of major sporadic 4-repeat tauopathies. To better define the astrocytic inclusions in PSP and CBD and to outline the pathological features of each disease, we reviewed 95 PSP cases and 30 CBD cases that were confirmed at autopsy. TAs exhibit a radial arrangement of thin, long, branching accumulated tau protein from the cytoplasm to the proximal processes of astrocytes. APs show a corona-like arrangement of tau aggregates in the distal portions of astrocytic processes and are composed of fuzzy, short processes. Immunoelectron microscopic examination using quantum dot nanocrystals revealed filamentous tau accumulation of APs located in the immediate vicinity of the synaptic structures, which suggested synaptic dysfunction by APs. The pathological subtypes of PSP and CBD have been proposed to ensure that the clinical phenotypes are in accordance with the pathological distribution and degenerative changes. The pathological features of PSP are divided into 3 representative subtypes: typical PSP type, pallido-nigro-luysian type (PNL type), and CBD-like type. CBD is divided into three pathological subtypes: typical CBD type, basal ganglia- predominant type, and PSP-like type. TAs are found exclusively in PSP, while APs are exclusive to CBD, regardless of the pathological subtypes, although some morphological variations exist, especially with regard to TAs. The overlap of the pathological distribution of PSP and CBD makes their clinical diagnosis complicated, although the presence of TAs and APs differentiate these two diseases. The characteristics of tau accumulation in both neurons and glia suggest a different underlying mechanism with regard to the sites of tau aggregation and fibril formation between PSP and CBD: proximal-dominant aggregation of TAs and formation of filamentous NFTs in PSP in contrast to the distal-dominant aggregation of APs and formation of less filamentous pretangles in CBD.

Key words: astrocytic plaque, corticobasal degeneration, fibril formation, progressive supranuclear palsy, tufted astrocyte.

INTRODUCTION

Progressive supranuclear palsy (PSP)[1] and corticobasal degeneration (CBD)[2] have been regarded as distinct clinicopathological entities with hyperphosphorylated four repeat (4R) tau aggregation in neurons and glia, although the recent recognitions of many clinical similarities have increasingly raised more difficulties in the clinical diagnosis of these two disorders. However, microscopic cellular tau pathology has been used to distinguish PSP from CBD.[3–5] PSP is defined primarily by tau-positive neurofibrillary tangles (NFTs), coiled bodies, threads, and tufted astrocytes, in contrast to the ballooned neurons, pretangles, threads, and astrocytic plaques that are characteristic of CBD (Table 1). Because PSP and CBD frequently present similar pathological distributions (Table 1, Fig. 1), a pathological diagnosis may be difficult without the discrimination of abnormal tau inclusions and particularly of the most characteristic and obvious tau morphology, that of astrocytic inclusions.[6] Therefore, it is important to reevaluate and differentiate between tufted astrocytes (TAs) and astrocytic plaques (APs) and to discuss the pathogenesis of these types of inclusions. To address these issues, we reviewed the morphology and differential distribution of

Correspondence: Yoshida Mari, MD, PhD, Institute for Medical Science of Aging, Aichi Medical University, 1-1 Yazakokarimata, Nagakute, Aichi 480-1195, Japan. Email: myoshida@aichi-med-u.ac.jp

Received 16 April 2014; revised 15 June 2014 and accepted 15 June 2014.

Table 1 Diagnostic pathological findings in progressive supranuclear palsy (PSP) and corticobasal degeneration (CBD)

	PSP	CBD
Lesion	Distribution	
Neuronal loss & gliosis	Affected cortices (variable)	Affected cortices/subcortical white matter (gliosis)
	Globus pallidus	Globus pallidus (variable)
	Subthalamic nucleus	Subthalamic nucleus (variable)
	Substantia nigra	Substantia nigra
		Striatum (caudate and putamen) (gliosis)
	Brainstem tegmentum	Brainstem tegmentum (variable)
	Dentate nucleus	Dentate nucleus (variable)
	Pons and medulla (variable)	Pons and medulla (variable)
Ballooned or achromatic neurons		Affected cortices
Gallyas/4R-tau positive lesions		
Neuronal inclusions	NFTs > Pretangles	Pretangles >> NFTs
	Substantia nigra, oculomotor complex, locus ceruleus, pons, brainstem nuclei, dentate nucleus, globus pallidus, subthalamic nucleus	Affected cortices, substantia nigra, globus pallidus, subthalamic nucleus
	Striatum, thalamus, basal nucleus of Meynert	Striatum, thalamus, basal nucleus of Meynert
	Affected Cortices (variable)	Brainstem nuclei and dentate nucleus
	Spinal cord	Spinal cord
Threads and coiled bodies	Threads and coiled bodies	Threads >> coiled bodies
	Brainstem, cerebellar white matter, globus pallidus, subthalamic nucleus, striatum, thalamus, gray matter and white matter, spinal cord	Subcortical white matter and gray matter, globus pallidus, subthalamic nucleus, striatum, thalamus, brainstem, spinal cord
Astrocytic inclusions	Tufted astrocytes	Astrocytic plaques
	Affected cortices, striatum, brainstem	Affected cortices, striatum

4R-tau, 4 repeat tau; NFTs, neurofibrillary tangles.

pathologic lesions of 95 neuropathologically confirmed PSP cases and 30 CBD cases that were registered at the Institute for Medical Science of Aging, Aichi Medical University. Our focus was on the pathogenesis of astrocytic inclusions, their disease specificity, and their morphological variations.

PROGRESSIVE SUPRANUCLEAR PALSY (PSP)

PSP is a progressive neurodegenerative disorders, described by Steele, Richardson and Olszewski in 1964.[1] It is the second most common form of parkinsonism after Parkinson's disease. Clinical features include abnormal gait, and postural instability, and recurrent falls, supranuclear ophthalmoparesis, cognitive and behavioral changes, pseudobulbar features and dystonia.

Clinical aspects

As noted previously, pathologically confirmed cases of PSP have exhibited some variation of the clinical and pathological features. Therefore, clinical subtypes were proposed to classify PSP: PSP-Richardson, PSP-parkinsonism (PSP-P),[7,8] PSP-pure akinesia with gait freezing (PSP-PAGF),[9] PSP-primary progressive aphasia,[10,11] and PSP-predominant cerebellar involvement (PSP-C).[12,13] The PSP-Richardson type is the prototypical form of PSP that is defined by early falls, early cognitive dysfunction, abnormalities of gaze and postural instabilities. PSP-P represents asymmetric onset, tremor, early bradykinesia, non-axial dystonia and a response to levodopa. Individuals with PSP-PAGF present with the gradual onset of freezing of gait or speech, absent limb rigidity and tremor, a lack of sustained response to levodopa, and no dementia or ophthalmoplegia in the first 5 years of disease. PSP-primary progressive aphasia is defined by the presence of primary progressive aphasia, or progressive nonfluent aphasia. Individuals with PSP-C develop cerebellar-predominant ataxia as the initial and principal symptom.

Neuropathology

Neuropathological diagnostic criteria

The pathological criteria for the diagnosis of PSP are well established and include specific neuronal loss with gliosis and neurofibrillary tangles (NFTs) in the subcortical and brainstem nuclei and in the cerebellar dentate nucleus with the pathological accumulation of abnormally phosphorylated microtubule-associated protein tau into filamentous deposits.[14] The NINDS diagnostic criteria for PSP and related disorders are pertinent for typical PSP,

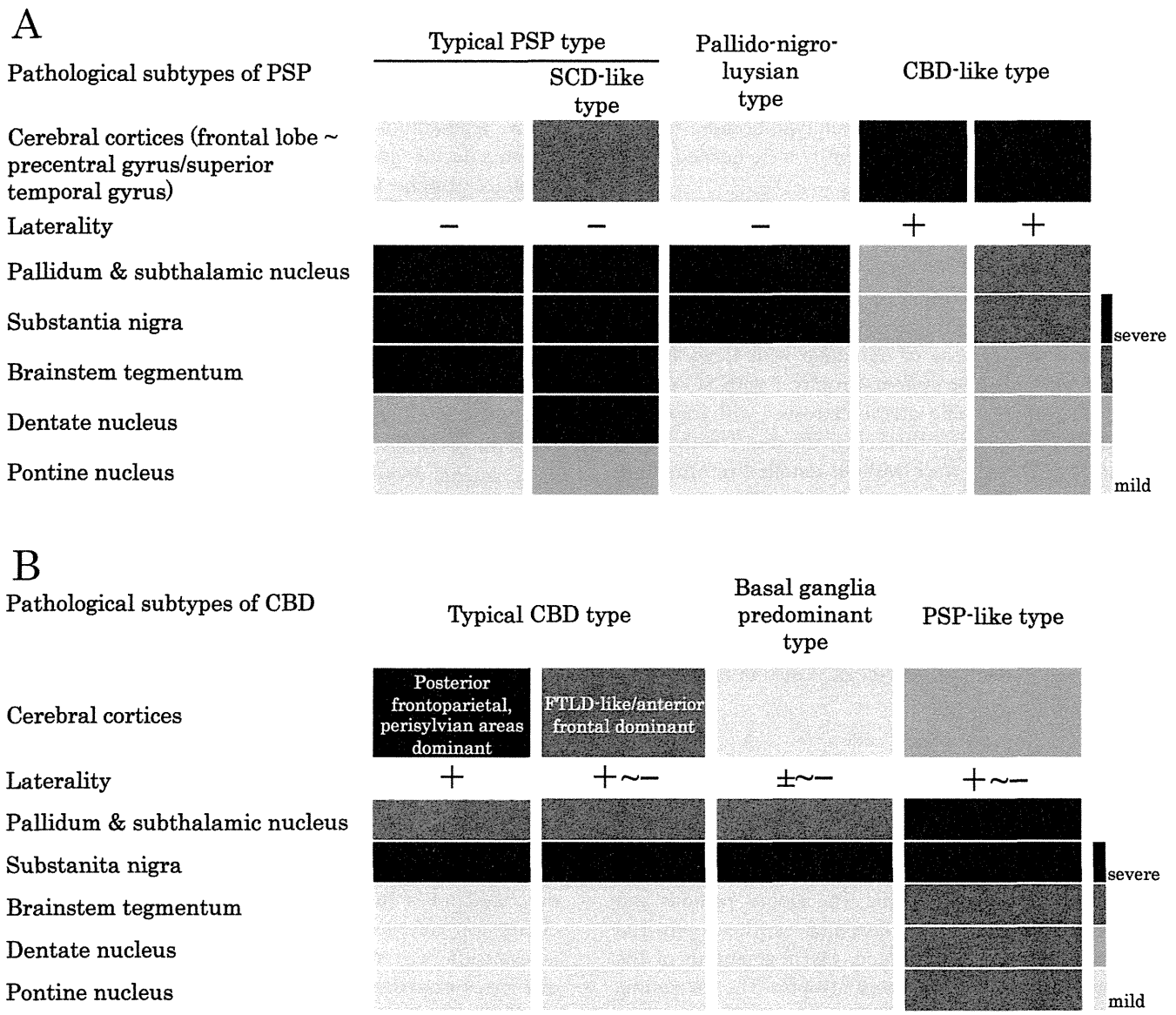

Fig. 1 The group of pathological subtypes in PSP (A) and CBD (B). (A) The pathological subtypes in PSP is generally divided into three representative types: typical PSP type, pallido-nigro-luysian type (PNL type), and CBD-like type, according to the distribution of the lesions and the severity. The spinocerebellar degeneration (SCD)-like type is associated with severe degeneration of the dentate nucleus, superior cerebellar peduncles, cerebellar cortex, white matter and pontine tegmentum and base, which are frequently associated with frontal involvement. The PNL type shows relatively restricted changes in pallido-nigro-luysian lesions. The CBD-like type is accompanied by more severe, asymmetrical cortical changes and a variable degeneration of the basal ganglia, brainstem and cerebellar dentate nucleus. (B) The pathological subtypes of CBD is generally divided into three representative types: typical CBD type, basal ganglia-predominant type, and PSP-like type, according to the distribution of the lesions and the severity. The typical CBD type shows dominant cortical involvement with laterality in the posterior frontoparietal or perisylvian areas. Some cases exhibit anterior frontal-dominant cortical degeneration, such as frontotemporal lobar degeneration. The basal ganglia-predominant type reveals severe involvement of the pallidum and subthalamic nucleus, with relatively mild cortical degeneration without distinct laterality. The PSP-like type shows severe degeneration of the brainstem and dentate nucleus similar to that seen in PSP, in addition to the variable cortical involvement.

which conforms to the original description, and atypical PSP, which consists of histologic variants where the severity or distribution of abnormalities, or both, deviate from the typical pattern; these criteria are also relevant for combined PSP, in which typical PSP is accompanied by concomitant infarcts in the brainstem, basal ganglia, or both.[3,12] Microscopic findings include a high density of NFTs and neuropil threads in at least three of the following areas: the pallidum, subthalamic nucleus, substantia nigra, or pons. In addition, a low to high density of NFTs or neuropil threads is found in at least three of the following areas: the striatum, oculomotor complex, medulla, or dentate nucleus. A clinical history

that is compatible with PSP is also required for diagnosis according to this set of criteria. These criteria have come to define the typical clinicopathological PSP cases. However, based on these criteria, it was recommended that atypical PSP should be excluded as a PSP subtype because further neuropathological studies of this entity were needed.

Neuropathological reevaluation of PSP cases

Among 95 pathologically confirmed PSP cases, 25 cases were associated with other significant diseases. Two of these cases were associated with Alzheimer's disease, 12 with Parkinson's disease or dementia with Lewy bodies (DLB), 1 with multiple system atrophy, 1 with SCA6 and DLB, 1 with amyotrophic lateral sclerosis, 1 with traumatic brain injury, 4 with cerebrovascular disease, 1 with glioblastoma, and 2 cases were without detailed information. With the exception of these 25 cases, 70 cases were analyzed and had the following characteristics: a mean age at onset of 67 years (range 39–92 years), a mean disease duration of 8 years (range 1–28 years), and a mean age at death of 75 years (range 49–106 years). PSP is a sporadic disease, although approximately 7% of affected individuals have a family history of neurological disorders, including parkinsonism or dementia.

Macroscopic and microscopic findings

The macroscopic examination of the brain in typical PSP reveals mild frontal atrophy including precentral gyrus, particularly in the convexity (Fig. 2A). The brainstem and cerebellum are mildly atrophic. The globus pallidus and subthalamic nucleus usually show a brownish atrophy. The third ventricle may be enlarged. The tegmentum of the midbrain and pons also shows atrophy. The substantia nigra shows discolored, while the locus ceruleus is often relatively preserved. The cerebellar dentate nucleus, and the superior cerebellar peduncle are atrophic.

The microscopic findings indicate neuronal loss and gliosis with NFTs, which appear globose in appearance, in the basal ganglia, thalamus, brainstem, and cerebellum (Table 1, Fig. 3). The thalamus has mild to moderate neuronal loss and gliosis, while the putamen and the caudate show mild gliosis. The most affected nuclei are the globus pallidus, subthalamic nucleus and substantia nigra. The affected regions of the brainstem are as follows: midbrain tegmentum including the superior colliculus, periaqueductal gray matter, oculomotor nuclei, locus ceruleus, pontine tegmentum, pontine nuclei, medullary tegmentum and the inferior olivary nucleus. The dentate nucleus usually exhibits grumose degeneration. The superior cerebellar peduncles are atrophic, and the cerebellar cortex may show mild loss of Purkinje cells with mild atrophy of the white matter. The medullary tegmentum may be atrophic with myelin pallor. The cerebral cortices show mild gliosis especially in the premotor and precentral gyrus in the convexity. The spinal cord, especially the cervical segment, is usually involved, particularly in the medial division of the anterior horn and intermediate gray matter.[15–17] Transverse sections of the spinal cord often show myelin pallor in the anterolateral funiculus in the cervical and thoracic segments. Immunohistochemistry for phosphorylated tau or modified Gallyas silver staining reveals NFTs, pretangles in neurons, tufted astrocytes, coiled bodies in oligodendrocytes, and threads (Table 1, Fig. 3).

Tufted astrocytes

TAs are defined as radial arrangements of thin and long branching fibers without collaterals that course continuously through the cytoplasm to the distal processes of astrocytes (Fig. 3d–j,m,n).[6,18] "Tufts of abnormal fiber," as described in PSP by Hauw *et al.*,[19] is the root of the nomenclature for "tufted astrocytes," although their cellular characterization was not mentioned in their study. Tufted astrocytes were described by Hauw *et al.*[19] as star-like tufts of fibers devoid of degenerative features and without amyloid cores that are clearly distinguishable with Bodian stain as well as with tau immunocytochemistry. The astrocytic nature of the cells that contain the tufted-type inclusions was confirmed by the double-labeling of sections with antibodies to GFAP, CD44 and abnormal tau.[20–22] Cytoplasmic staining is usually not conspicuous within TAs

Fig. 2 Macroscopic findings of typical PSP type (A), pallido-nigro-luysian (PNL)- type (B) and CBD-like type (C).
(A) Macroscopic findings in coronal sections of typical PSP show mild frontal atrophy in the convexity (a), atrophy of the pallidum and subthalamic nucleus (a, arrow), atrophy of the brainstem tegmentum (b), loss of pigment in the substantia nigra (b, arrow) with preservation of pigment in the locus ceruleus, and atrophy of the cerebellar dentate nucleus (c). Bar = 2 cm.
(B) Macroscopic findings in PNL-type PSP reveal severe atrophy of the pallidum and the subthalamic nucleus (a) and depigmentation of the substantia nigra (b), with relative preservation of the brainstem tegmentum (b) and cerebellar dentate nucleus (c). The PNL-type sometimes shows atypical TAs, which demonstrates proximal dominant tau accumulations (d, e). d, Gallyas silver stain; e, AT8 immunohistochemistry; a, b, c, bar = 2 cm; e, bar = 10 μm.
(C) Macroscopic findings in CBD-like type PSP indicate left side-predominant degeneration of the cerebral cortices and the basal ganglia (a–d) with relatively mild atrophy of the brainstem (e). Microscopically typical TAs are observed in the basal ganglia and cerebral cortices (f, g). a, c, Klüver-Barrera stain; b, d, Holzer stain; f, Gallyas silver stain; g, AT8 immunohistochemistry; bar = 10 μm.